

Proposal of an optimal experimental method for evaluation of the concrete shear transfer mechanism

Y. Takase & M. Ueda

Hokkaido University, Hokkaido, Japan

T. Wada

Dept. of Architecture, Hokkaido Polytechnic College, Hokkaido, Japan

ABSTRACT: In this study, a new experimental method has been proposed in order to evaluate shear transfer mechanism of cracked concrete. For the purpose of controlling transition of crack width under shear stress mode precisely and automatically, tetra-axes loading system based on optimal control theory and PID (proportional, integral, derivative) algorithms was used for controlling. As the results, it is proved that this kind of experiments should be controlled not manually but automatically for the accuracy. Moreover, the experimental data obtained by using this system and also identify the optimal PID values for the experiments.

1 INTRODUCTION

When shear force cause slip deformation in the horizontal direction along the concrete crack surface (hereinafter: shear deformation), stress is transferred by contacting micro crack surfaces. This phenomenon is called shear transfer mechanism. In assessing the load and deformation responses of steel reinforced concrete members, it is extremely important to clarify this mechanism.

The significance of this phenomenon is widely known, and previous experimental studies have aimed to clarify the phenomenon. Unfortunately, different loading and measurement methods among researchers have made it difficult to compare their test results.

The main reason for this is conceived to be as follows: With the progression of shear deformation, the contact action between crack surfaces is sensitive to the effects from loading conditions; i.e., the loading control method and its precision. However, all previous test systems appear to have problems in the loading control method and its precision from the author's point of view.

Under the current state of research as mentioned above, the authors developed a new crack surface precise control type shear loading system, to clarify the shear stress transfer mechanism. This paper provides an overview of a loading device developed by the authors that operates by tetra-axial loading, and it explains the devices automatic control method, which is based on proportional-integral-derivative (PID) control theory. Together with this, the aim of this paper is to verify the functionality of this system

and to identify the optimum PID control parameters by using this loading system and studying the results of tests performed on 14 concrete crack test specimens.

2 LOADING TEST

2.1 Loading equipment

Testing of the shear stress transfer on the concrete crack surface requires a loading test device that al-

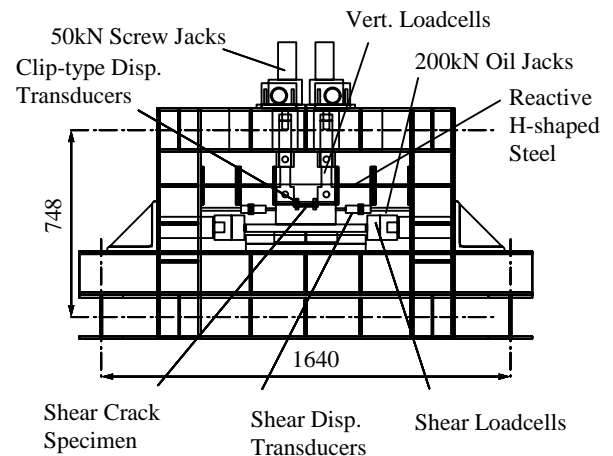


Fig. 1. Loading jack and frame of the testing device

Table 1. Performance of servo system

| Servo Aparatus | Max. Speed | Max. Output |
|----------------|------------|-------------|
| Motor | 4500 r/min | 2.88 N·M |
| Speed Reducer | 180 r/min | 12.75 N·M |
| Screw Jack | 0.5 mm/sec | 50 kN |

lows loading in two directions: the shear direction and the vertical direction to the crack surface.

Figure 1 shows the loading jack and frame of the testing device. Figure 2 shows its control and measurement system. This testing device is equipped with two 200-kN hydraulic jacks for applying shear force, and four 50-kN servo screw jacks in the vertical direction, which allows the precise manipulation of crack widths. Table 1 shows the performance of the servo system mechanism.

2.2 Test specimen

Figure 3 shows the dimensions of the specimen used to test shear stress transfer (hereinafter: the test specimen), and Figure 4 shows the details of the steel fastening device (hereinafter: the steel cap) used to fasten the test specimen to the test device. Table 2 shows the concrete mix, and Table 3 shows the material properties. The test specimen is a 95mm x 160mm x 250 mm rectangular solid.

Notches were cut at the four sides of its periphery to initiate and produce a crack surface area of 7500 mm². Based on previous tests by the authors, the size (scale) of the crack surface area was made sufficiently large to produce a crack with constant roughness.

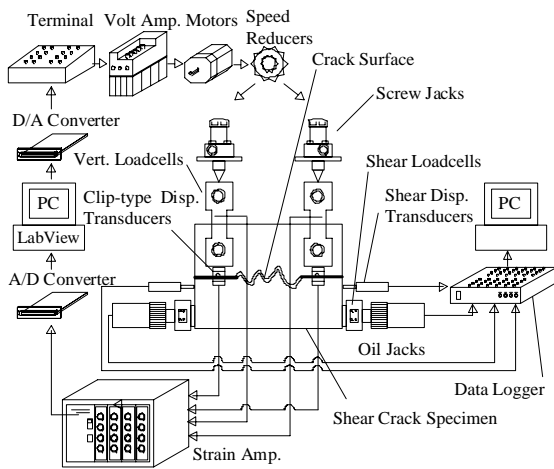


Fig.2. Details of crack surface precise control type shear loading system

Table 2. Concrete mix

| W/C (%) | Mix (kg/m ³) | | | | |
|---------|--------------------------|--------|------|------|--------|
| | Water | Cement | Agg. | Sand | Admix. |
| 38.5 | 176 | 458 | 787 | 880 | 4.992 |

Table 3. Concrete properties

| Max. Aggregate | Comp. Strength | Tensile Strength |
|----------------|------------------------|------------------------|
| 20 mm | 39.2 N/mm ² | 3.22 N/mm ² |

Table 4. Performances of sensors

| Sensors | Direction | Rated Capacity | Rated Output mV/V |
|--------------|-----------|----------------|-------------------|
| Displacement | Shear | 25 mm | 6.25 |
| Load Cell | Shear | 200 kN | 2.5 |
| Displacement | Normal | 2 mm | 2.5 |
| Load Cell | Normal | 50 kN | 0.28 |

The steel cap in Figure 4 was used for connecting the test specimen to the loading frame. One steel cap was bolted at the top of the test specimen and another was bolted at the bottom of it, then the space created in between was filled with shrinkage-compensating cement to bind them into a single structure.

2.3 Gauges for displacement and stress

The physical values that are essential for clarifying the shear transfer mechanism are shear displacement (δ), crack width (ω), shear stress (τ), and normal stress (σ). Table 4 lists the devices used to measure these four physical values.

In this study, the test specimen is separated at the crack into an upper and a lower block. Displacement between the upper and lower blocks in the shear direction was measured with a displacement transducer (25 mm), and the relative difference between the blocks is the shear displacement δ . Crack width ω is measured using clip type displacement transducer and according to the spread at the tip of copper elements that are bonded to the crack surface at four points.

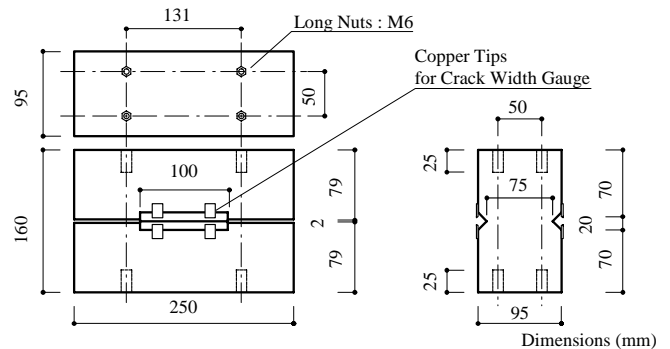


Fig.3. Dimensions of test specimen

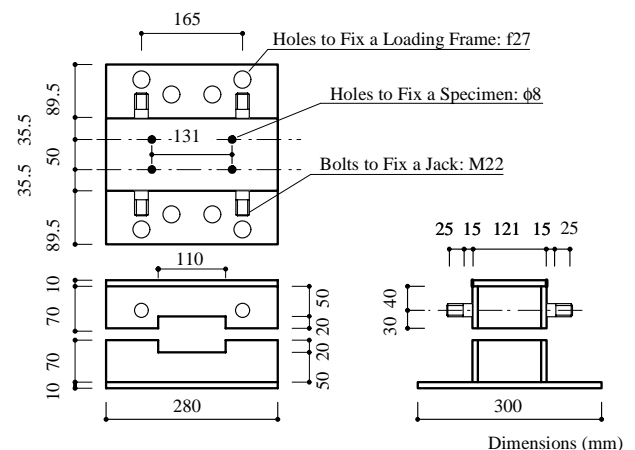


Fig.4. Dimensions of steel caps

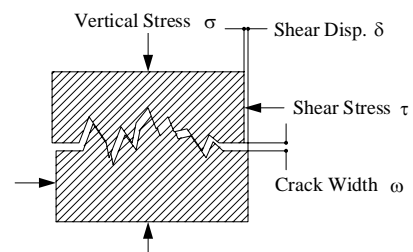


Fig.5. Mechanism of shear transfer on crack surface

Shear stress τ is calculated by first measuring with a 200-kN load cell installed at the loading point of the hydraulic jack, and then by dividing the load value with the area of the crack surface. Similarly, normal stress σ is calculated by obtaining the total load on four points and dividing this by the area of the crack surface.

2.4 Control system and theory

The load actuator in this study has a dual system for controlling the load in the shear and vertical directions. Shear force is applied to the test specimen manually by the operator, and the resulting crack width deviations at the four points are adjusted with the vertical control system of the tetra-axial automatic control mechanism.

The automatic measurement and control system for the vertical direction is constructed with the LabVIEW system. The A/D-D/A converter is capable of 16-bit resolution at a sampling interval of 12.5 Hz.

PID control theory, the advantages of which is versatility and generality, was used for controlling the crack width. This is because there are wide variations in the concrete crack surfaces of the test specimens, and therefore, coordination in measuring, controlling and loading became very complicated.

The transfer function in PID control theory is shown in the equation below, with error $e(s)$, the difference between input value (crack width ω) and target value (ω_0), as the basic variable. The transfer functions for the four corner points on the crack surface are assumed to be independent.

$$U(s) = K_p \cdot \left[1 + \frac{1}{T_i \cdot s} + T_D \cdot s \right] \cdot e(s) \quad (1)$$

Whereby, s : Laplace operator, $U(s)$: output voltage, $e(s)$: error, K_p : proportional gain, T_i : integral time, and T_D : derivative time.

3 TEST RESULTS

This section studies the effects over test results from PID control parameter values that are for applying tetra-axial load onto crack width. Before performing the automatic control test, the limitations of manual control were clarified by performing tests in which the crack width was controlled manually.

3.1 Outline of the test

Table 5 lists the test specimens. One test specimen for manual control and 13 test specimens for automatic control were produced. A common condition for all test specimens is that crack width ω is kept

constant. This condition is the target crack width ω_0 (Table 5). To verify the three parameters of PID control, the P-series, I-series, and D-series of tests were performed.

The test specimens were given designations according to their specifications. The number that follows the first letter W indicates the target crack width ω_0 , followed by the parameter values for the proportional, integral and derivative (P, I, D) actions. According to PID control theory, the proportional action is known to be the most effective; therefore, proportional gain K_p was introduced into all test specimens.

The control parameter was verified using the ultimate sensitivity method, which is common in the field of automatic control. This test device was designed to allow the controlling of crack widths in the range of 0.1 mm to 1.0 mm; therefore, the standard crack width in this test was approximately the median value of 0.5 mm.

The loading test procedure is described hereafter. First, the test specimen is set on the test device, and the crack surface is made by directly applying tensile force. Then, with the test specimen placed on the test device, horizontal shear force was applied while the target crack width ω_0 was maintained by the aforementioned automatic control method.

3.2 Results from the manual control test

Figure 6 shows the displacement and stress of test specimen W05MNU. Each of the four jacks that manipulate crack width has an operator in charge. There was another operator for the shear loading jack and one person in charge of measurement. The test was performed with six persons, who need to be sufficiently skilled in their operations.

Table 5. Lists of the test specimens

| Specimen | Series | Control | ω_0 (mm) | K_p | T_i | T_D |
|------------|--------|-----------|-----------------|-------|-------|-------|
| W05MNU | MNU | Mnual | 0.5 | - | - | - |
| W05P10 | P | Automatic | 0.5 | 10 | - | - |
| W05P40 | P | Automatic | 0.5 | 40 | - | - |
| W05P60 | P | Automatic | 0.5 | 60 | - | - |
| W05P120 | P | Automatic | 0.5 | 120 | - | - |
| W01P60 | P | Automatic | 0.1 | 60 | - | - |
| W10P60 | P | Automatic | 1.0 | 60 | - | - |
| W10P120 | P | Automatic | 1.0 | 120 | - | - |
| W05P60I100 | I | Automatic | 0.5 | 60 | 100 | - |
| W05P60I40 | I | Automatic | 0.5 | 60 | 40 | - |
| W05P60I10 | I | Automatic | 0.5 | 60 | 10 | - |
| W05P60D01 | D | Automatic | 0.5 | 60 | - | 0.1 |
| W05P60D02 | D | Automatic | 0.5 | 60 | - | 0.2 |
| W05P60D03 | D | Automatic | 0.5 | 60 | - | 0.3 |

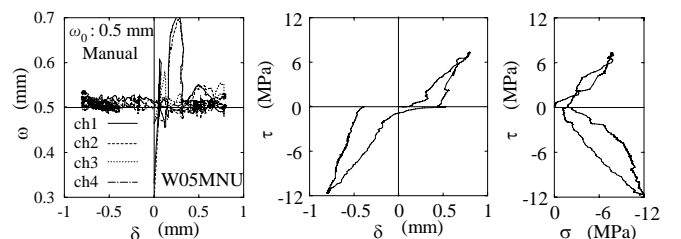


Fig.6. Results for W05MNU

The target value (crack width) was $\omega_0 = 0.5$ mm, but the crack width - shear displacement curve on the left side of Figure 6 shows a maximum displacement of 0.2 mm, which is an error of almost 40% of the target value. Once the error in controlling crack width increases, its effect on the non-linearity (plasticity) of the crack surface becomes significant and could render the test meaningless.

The above result clarified that manual control of crack width is impossible.

3.3 Results of the PID automatic control test

3.3.1 Results for P-series tests

This section verifies the degree of effect that proportional gain K_P , which is the most effective of the three PID control parameters, has in controlling crack width.

(1) When $\omega_0 = 0.5$ mm

Figures 7(a) to 7(d) show the results for test specimens W05P10, W05P40, W05P60, and W05P120 when the test parameter is the proportional gain K_P and the parameter values are changed in four stages: 10, 40, 60, and 120. Figures 7(a) to 7(d) also show the curves for crack width ω - shear displacement δ , shear stress τ - shear displacement δ , and shear stress τ - normal stress σ . The $\omega - \delta$ curves in all these figures show crack width values that were measured at the four corners of the crack surface.

With test specimen W05P10 in Figure 7(a), where the proportional action was set at minimum, the crack width ω did not fully converge with the target value ω_0 (0.5 mm). Furthermore, the curves of other stresses showed gently curves.

In the results from test specimens W05P40, W05P60, and W05P120, where a higher value for the proportional gain K_P was set, the crack widths converged at about 0.5 mm and the $\tau - \sigma$ curves showed mutually similar tendencies. An apparent characteristic of these curves is that it has a sharp turn-around point when unloading.

The above verification shows that proportional action is highly effective in elucidating the displacement and stress at the shear crack surface when the target crack width is 0.5 mm. It also became clear that precise test results could be obtained by setting the proportional gain K_P within the range of 40 to 120.

(2) When $\omega_0 = 0.1$ and 1.0 mm

The previous section showed that proportional gain K_P is effective for adjusting the crack width when the target crack width is 0.5 mm. However, K_P is expected to differ in effectiveness when the target crack width differs from the standard value of 0.5mm. This section studies how proportional gain

K_P affects when the target crack width was changed to 0.1 mm and to 1.0 mm.

Figure 8(a) shows the displacement and stress from the W01P60 test specimen when the crack width is 0.1 mm and $K_P = 60$. In this test, the test specimen with a target crack width of 0.1 mm showed the highest aggregates interlock and prominent dilatancy. Figure 8(a) shows that the crack width satisfies the target value. Although there was some residual normal stress near the point of origin, the overall changes in displacement and stress could be understood from the shear stress - normal stress curve.

Figure 8(b) shows the displacement and stress in specimen W10P60 when the target crack width ω_0 is 1.0 mm and the proportional gain $K_P = 60$. From this figure, changes in crack width and shear stress seem stable. However, vibrating changes in normal stress could be observed. The proportional gain K_P was raised from 60 to 120, and the results for specimen W10P120, with maximum speed for correcting deviation, are shown in Figure 8(c). In this figure, the crack width remains constant and changes in stress show a continuous curve with little turbulence.

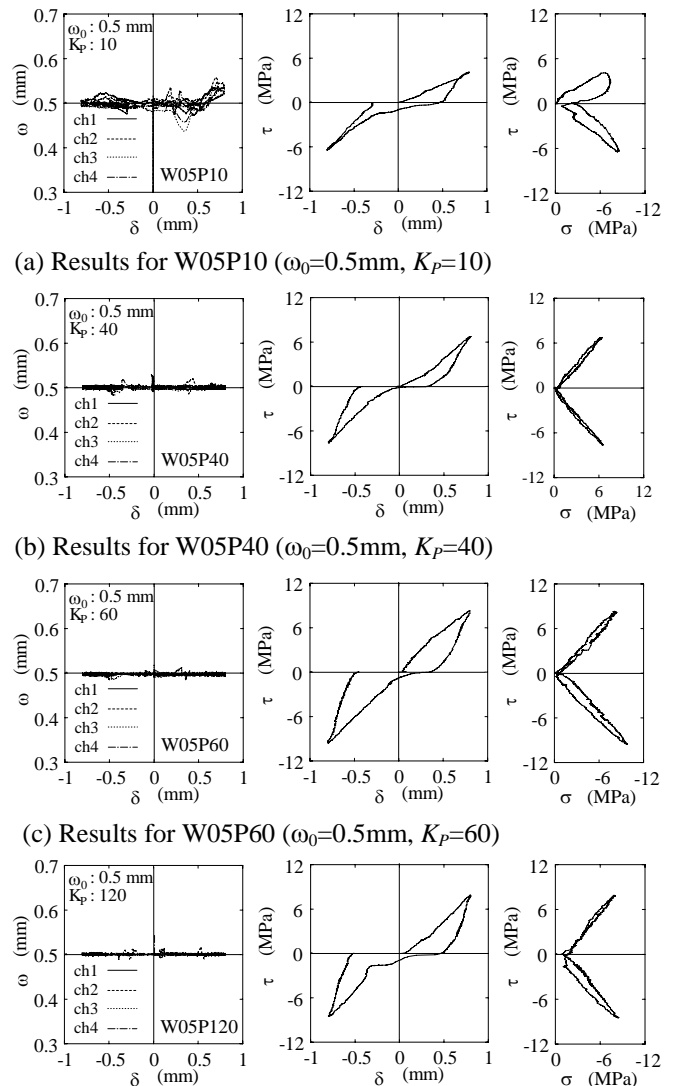
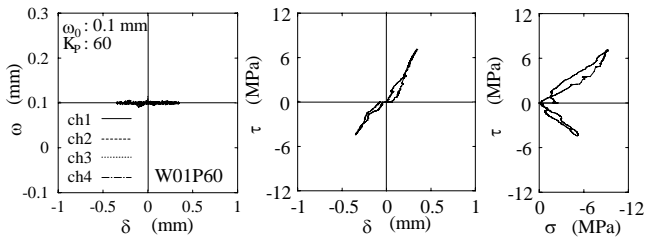
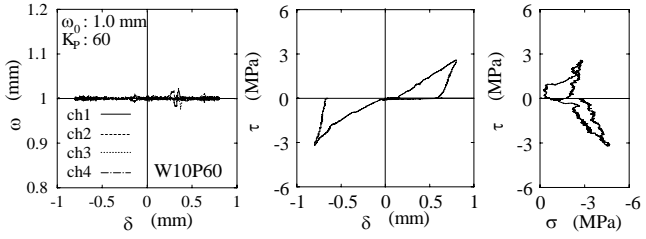


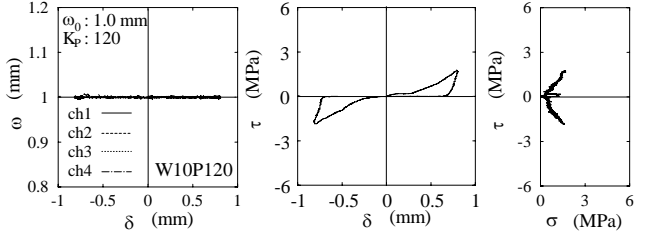
Fig.7. P Sires ($\omega_0=0.5$ mm)



(a) Results for W01P60 ($\omega_0=0.1\text{mm}$, $K_p=60$)

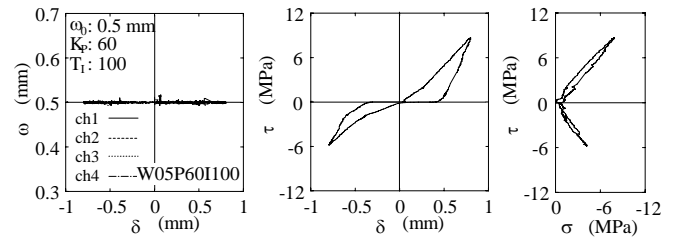


(b) Results for W10P60 ($\omega_0=1.0\text{mm}$, $K_p=60$)

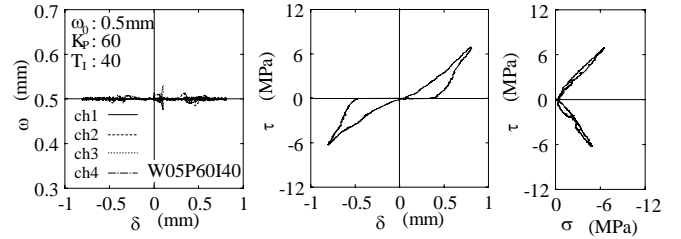


(c) Results for W10P120 ($\omega_0=1.0\text{mm}$, $K_p=120$)

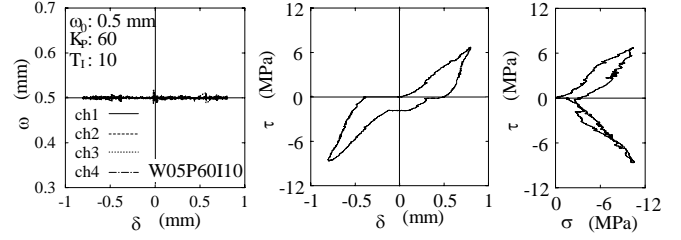
Fig.8. P Sires $\omega_0=0.1, 1.0\text{mm}$



(a) Results for W05P60I100 ($\omega_0=0.5\text{mm}$, $K_p=60$, $T_I=100$)



(b) Results for W05P60I40 ($\omega_0=0.5\text{mm}$, $K_p=60$, $T_I=40$)



(c) Results for W05P60I10 ($\omega_0=0.5\text{mm}$, $K_p=60$, $T_I=10$)

Fig.9. I Sires ($\omega_0=0.5\text{mm}$, $K_p=60$)

3.3.2 Results for I-series tests

In automatic control, integral action was introduced to improve the steady-state error (error that resides constantly) or to adjust the accuracy of error. It is the integral time T_I that controls this integral action, and as clarified by PID equation (1) mentioned above, the control output $U(s)$ increases as the T_I decreases. In the verification of proportional action that was described in the previous section, steady-state error was not identified. The present section studies the effects of integral action when the integral time T_I changes in three stages of 100, 40, and 10.

Figures 9(a) to 9(c) show the test results for test specimens W05P60I100, W05P60I40 and W05P60I10 with T_I as the test parameter.

In Figure 9(a), test specimen W05P60I100 has the largest T_I , and therefore, the smallest integral action. As for the P-series test specimen W05P60 in Figure 8(c) of the previous section, the resulting curve was very stable.

In Figure 9(b) where the integral time $T_I = 40$, and in Figure 9(c) where $T_I = 10$, both crack widths ω satisfy the target value. However, the shear stress - normal stress curve is clearly affected by the integral action, whereby the $\tau - \sigma$ curve shows minor but intense local increases and decreases, and the entire curve appears to be unstable.

The instability of the test response values, caused by the integral action shown in Figures 9(a) to 9(c), is attributed to the following reasons. To correct the error from a certain target value that was measured with the integral action according to T_I , an output of

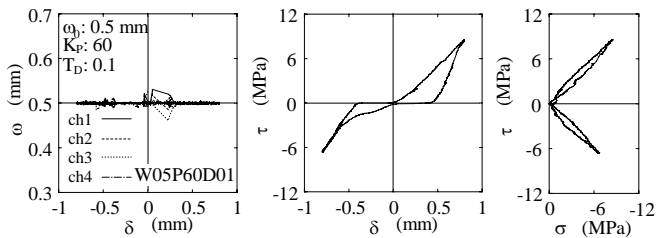
response that surpasses the target value will continue to produce an opposite error. As a result, the undulating measured value will converge with the target value in the end. In this test, this action is not clearly observed from the $\omega - \delta$ curve, which shows the transition in crack width, but it was observed that this is sensitive to and is affected by normal stress. Therefore, it could be concluded that integral time T_I need not be incorporated in the system.

3.3.3 Results for D-series tests

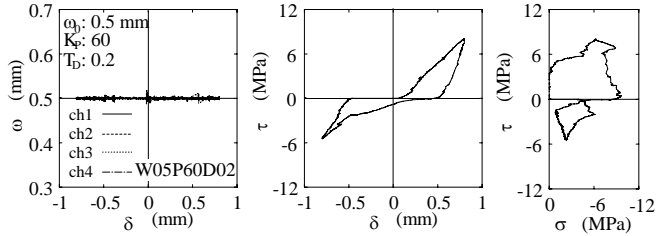
Readiness in controlling crack is anticipated from the derivative time T_D , which is the third independent variable in the previous equation (1). The D-series test verifies the effects on this loading test when the derivative time T_D , as the test parameter, changes in three stages from 0.1, 0.2 to 0.3. Figures 10(a) to 10(c) show the test results for the three test specimens W05P60D01, W05P60D02, and W05P60D03.

From the test results of specimen W05P60D01, with the derivative action set at the minimum value of 0.1, effects from the derivative action, such as improving the precision of the test value, have not been observed.

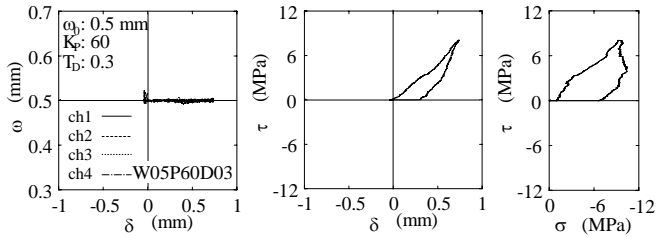
For test specimen W05P60D02 at $T_D = 0.2$, and W05P60D03 at $T_D = 0.3$, the crack width in both cases converges with the target value. However, the curve that shows the relation between shear stress τ and normal stress σ is very turbulent, and has lost its significance as a shear test. The highly turbulent normal stress was sensitive to the derivative action, which was assumed to be caused by electric noise



(a) Results for W05P60D01 ($\omega_0=0.5\text{mm}$, $K_p=60$, $T_D=0.1$)



(b) Results for W05P60D02 ($\omega_0=0.5\text{mm}$, $K_p=60$, $T_D=0.2$)



(c) Results for W05P60D03 ($\omega_0=0.5\text{mm}$, $K_p=60$, $T_D=0.3$)

Fig.10. D Sires ($\omega_0=0.5\text{mm}$, $K_p=60$)

that was not damped in this measurement system. The noise level was about several times more than the clip type displacement transducer measurement sensitivity of $1/2500$ mm, which indicates that electrical conditions in the environment could have significantly affected this.

From test specimen W05P60D03, there was excessive residual normal stress after unloading the force and the safety function in this system force-terminated the loadings.

From the results of the D-series tests, it was concluded that introducing derivative time T_D into this system is not necessary.

4 CONCLUSION

This research used a test device newly developed by the authors. The device has a tetra-axial loading mechanism to apply shear force to concrete crack surfaces. The test device has a high-precision automatic control system that is based on PID control theory to maintain constant crack widths.

The main objectives of this paper are to verify the functionality of this test device and to identify the optimum PID control parameters for shear slip tests on the concrete crack surface. The findings are as follows.

1 High-precision control of crack width was impossible to perform manually. Automatic control is essential.

2 High-precision control of crack width is possible by setting the proportional gain K_p between 60 and 120. Furthermore, with large crack widths, the proportional gain needs to be high.

3 Control by proportional action alone was sufficient for controlling the displacement of the crack surface, and integral or derivative actions were largely unnecessary.

4 The high-precision controlled loading system for testing crack surfaces that is proposed by the authors is expected to provide valuable information for clarifying the shear stress transfer mechanism on concrete surface.

ACKNOWLEDGEMENTS

We would like to express our gratitude to Mr. Tadao Narita of the Department of Control Technology, Hokkaido Polytechnic College, for his valuable advice, as well as to Mr. Masaaki Kibata, who is pursuing a Master degree at Hokkaido University, for his contributions.

REFERENCES

- Bujadham,B.1991.The Universal Model for Transfer across Crack in Concrete, Department of Civil Engineering, The Graduate School of The University of Tokyo
- Hasegawa,R.,Katori,K.,Shinohara,Y.,& Hayashi,S.2004.Shear Transfer Mechanism on the Crack surface in High Strength Concrete JCI Aniversal ,Vol.26,No2:91-96
- Li,B.,Maekawa,K.,& Okamura,H.1989.Contact Density Model for Stress Transfer across Cracks in Concrete.J.of the Faculty of Eng. University of Tokyo(B),Vol.40,No.1:9-52
- Mattok,A.H.1974.Shear Transfer In Concrete Having Reinforcement At An Angle To The Shear Plane, Publication SP-42 Shear in Reinforced Concrete, ACI:17-42
- Michael,N.Fardis,& Oral,B.1979.Shear Transfer Model for Reinforced Concrete, ASCE, Vol.105, No. EM2: 255~275
- Millard,S.G.& Johnson,R.P.1984.Shear Transfer across Cracks in Reinforced Concrete due to Aggregate Interlock and Dowel Action, M. of Concrete Research,Vol.36, No.126 : 123-137
- Nishimura,A.,Fujii,M.,Miyamoto,A.&Saito,I.1985.Effect of the Crack Surface Roughness on Shear Transfer at the Cracks in Reinforced Concrete Beams, J. of JSCE, No.360, V-3:91-100
- Sato,R.,Wada,T.,&Ueda,M.2001.Fast Fourier One-dimensional analysis of concrete crack surface, FRAMCOS-4:423-430
- Shinohara,y.,Kawamichi,K.& Ishitobi,S.2001.Shear Behavior in Precracked Concrete under Cyclic Loading at Constant Crack Width., J. Struct.Constr.Eng.,AIJ,No.548:101-106
- Van Mier, J.G.M., Nooru-Mohamed, M.B., & Timmers, G.1991.An experimental study of shear fracture and aggregate interlock in cement based composites, Heron, Vol.36 , No.4
- Wada,T.,Sato,R.,Ishikawa,C.&Ueda,M.1996.Development of Mesurement of the Concrete Crack Surface by Laser Beam and Proposal of 2-Dimensional Analytical Method of the Measured Image -A basic study on shape properties of the concrete crack surface Part.1-, J. Struct. Constr. Eng., AIJ, No.490:179-188

- Wada,T.,Sato,R.,Ishikawa,C.&Ueda,M.1998.2-Dimensional Shape Analysis of the Concrete Crack Surfaces Introduced by Various Kinds of Stress -A basic study on shape properties of the concrete crack surface Part.2-, J. Struct. Constr. Eng., AIJ, No.504:81-86
- Wada,T.,Sato,R.,Ishikawa,C.&Ueda,M.1999.Proposal of 3-dimensional analytical method for the concrete crack surface image measured by laser beam -A basic study on shape properties of the concrete crack surface Part.3-, J. Struct. Constr. Eng., AIJ, No.524:111-118
- Wada,T.,Sato,R.,Ishikawa,C.&Ueda,M.2000.3-dimensional shape analyses of the concrete crack surfaces introduced by various kinds of stress -A basic study on shape properties of the concrete crack surface Part.4-, J. Struct. Constr. Eng., AIJ, No.534:103-111
- Walraven.J.C.1981.Fundamental Analysis of Aggregate Interlock, ASCE, Vol.107, No. ST11:2245-2270